# Polarization and Droplet Size Effects in the Laser-Trapping-Induced Reconfiguration in Individual Nematic Liquid Crystal Microdroplets

Anwar Usman,* Wei-Yi Chiang, Takayuki Uwada, and Hiroshi Masuhara*

Department of Applied Chemistry and Institute of Molecular Science, National Chiao Tung University, Hsinchu 30010, Taiwan

ABSTRACT: We experimentally demonstrate reordering throughout the inside of an individual bipolar nematic liquid-crystalline microdroplet optically trapped by a highly focused laser beam, when the laser powers are above a definite threshold. The threshold depends on the droplet size and laser polarization. A physical interpretation of the results is presented by considering the nonlocal orientations of the nematic liquid-crystal molecules in the droplets with the dimensions on the order of the focal spot diameter or larger. On the basis of the finite size approximation, we show that the dependence of threshold power on the droplet size is calculated to be in qualitative agreement with the experimental data.

Linearly polarized laser beam

Circularly polarized laser beam
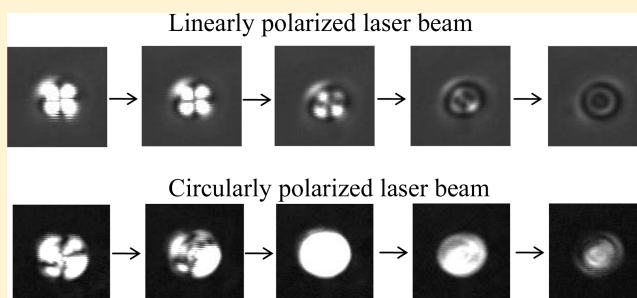
1. INTRODUCTION

An optical trapping technique that utilizes a tightly focused continuous-wave (cw) laser beam allows one to manipulate micrometer- or submicrometer-sized objects.[1,2] Therefore, this technique becomes indispensable and has been widely applied in particle deposition,[3−5] particle aggregations,[6,7] polymerization,[8] and crystallization.[9−12] In particular, the optical trapping-induced crystallization relates the focused light with three-dimensional molecular alignment that may involve many optical and physical phenomena, such as migration of molecules or clusters from the surrounding area to the focal spot and cooperative molecular realignment driven by the focused light. For specific cases, such phenomena have been demonstrated in the suspension of gold nanoparticles and in liquid crystal (LC) thin film, respectively.[13−15]

We should note that over the past 2 decades, electric-field-induced configurational transition of the LC droplet in polymer matrixes has been studied in detail in terms of geometry, shape, and temperature dependences.[16−18] On the other hand, optical-field-induced molecular reorientation of LC thin films as so-called optical Fréederickscz transitions (OFT) has been experimentally investigated,[19] and this phenomenon has been elucidated using an accurate quantitative theory[20] and numerical analysis[21] of transverse reorientation by either an infinite plane wave or a finite beam treatment. The optical realignments have also been revealed in spherical LC droplets with various kinds of self-organized configurations depending on droplet−liquid boundary conditions in the medium in which they were dispersed.[22−28] Typically, the trapping beam at low power densities can only induce conoscopic structures or rotation of the birefringent nematic LC droplets.[24,27] Similar phenomena were also observed for optically trapped bipolar nematic[22,23] or cholesteric LC droplets.[25,26]

To exemplify the laser-trapping-induced realignment throughout the inside of LC droplet, here we report how reordering can take place in optically trapped bipolar nematic LC droplets of 4′-pentyl-4-cyanobiphenyl (5CB) dispersed in heavy water (D_2O). In such a medium, the effects of local heating around the focal spot due to laser-induced temperature elevation can be suppressed as the temperature elevation in D_2O by 1064 nm laser irradiation has been reported to be 2.6 °C/W, an order of magnitude lower than that of H_2O (24 °C/W).[29,30] We found that the reordering takes place only when the laser power is above a definite threshold depending on the droplet size and polarization state. Typically, the reordering was observed as a transition from a Maltese cross to a ring pattern in cross-polarization light imaging. This suggests that the likely mechanism involves transverse nonlocal response of the nematic alignment of LC molecules to a highly focused laser beam. This phenomenon in LC thin films has been described in detail by several groups,[19] and the ring pattern has been attributed to the self-phase modulation.[31,32] We also confirmed this mechanism by showing that the dependence of the threshold power on the droplet size is in qualitative agreement with the experimental observation.

2. EXPERIMENTAL SECTION

2.1. Optical setup. A 1064 nm cw beam from a Nd:YVO$_4$ laser (Spectra Physics; J20I-BL-106C) was collimated and focused down with an UPlanApo oil-immersing objective lens (100×, NA = 1.35) at normal incidence into a sample cell, which was mounted on the microscope stage of an inverted microscope (Olympus IX71). The polarization state of the trapping beam was controlled by a half-wave and quarter-wave
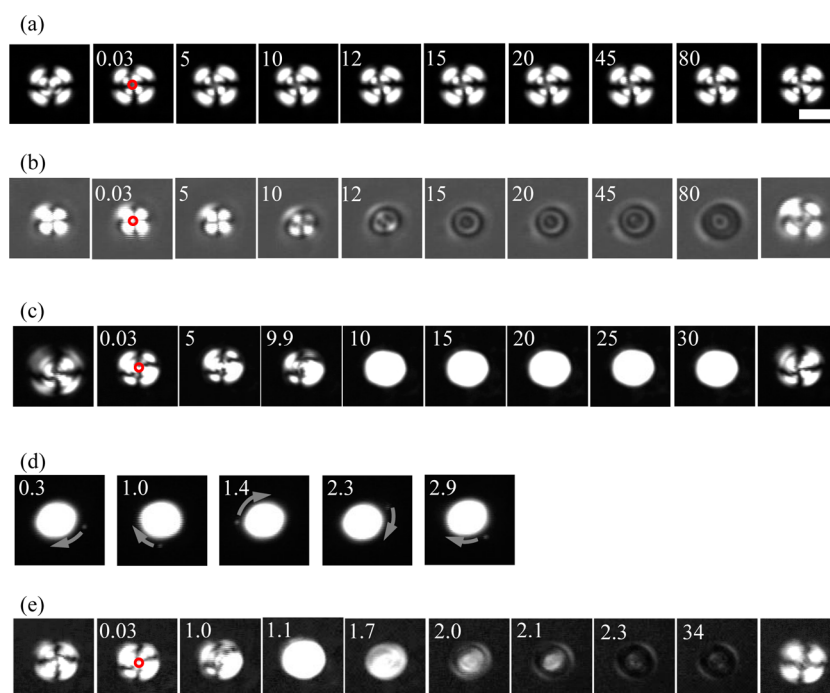
Figure 1. Sequences of time evolution of POM images of an individual bipolar nematic 5CB droplet optically trapped by a linearly polarized trapping beam at (a) 130 mW (or 54 MW/cm^2) and (b) 850 mW (or 360 MW/cm^2) and by a circularly (left-handed) polarized beam at (c) 460 mW (or 190 MW/cm^2) and (d) an orbit of a small droplet around the rotating optically trapped droplet (the time is in seconds after the droplet starts to rotate) and at (e) 940 mW (or 390 MW/cm^2). In panels (a–c) and (e), the trapping time (in second) is indicated in each snapshot, while the most left and most right snapshot in each sequence is the image just before the laser trapping beam is switched on and just after the beam is switched off, respectively. The red circles denote the focal spot area, and the scale bar of 3 μm is applied for all images.

plate. The beam waist of the focal spot was calculated to be 0.39 μm by using numerical analysis of Airy pattern. The laser power after the objective lens was varied in the range of 0.1– 1.0 W. The laser-trapping-induced reorientation inside of the LC droplet was analyzed conventionally by polarization optical microscopy (POM), which was performed by passing visible probe light from a halogen lamp (λ = 400−750 nm) through the pair of polarizers sandwiching the sample cell. Transmittance of the probe light was continuously detected by using a charge-coupled device (CCD) camera (JAI; CV-A55IR E) running at 30 interlaced frames per second. The elastic light scattering from the trapping beam was completely eliminated by a low-pass filter before the CCD camera.

2.2. Sample Preparation. The sample cell was assembled from two cover-glass plates (Matsunami). The thickness of the cell chamber (15−25 μm) was obtained by using the strips of parafilms along the glass edges, and the chamber was filled with 5CB (Tokyo Kasei Co.; the ordinary and extraordinary refractive indices are 1.54 and 1.74, respectively) suspended in D$_2$O (refractive index = 1.33) without the addition of any surfactants. The immiscible 5CB in D$_2$O spontaneously forms nematic droplets due to droplet−liquid interfacial tension,[28,33] and without the surfactant, the droplet adopts a polar-like (bipolar) molecular arrangement.[23,34] In the bipolar configuration, the molecules at the inside of the droplet are oriented similarly to the nematic orientation in the bulk, while the molecules at the droplet−liquid interface are oriented along the surface due to the so-called anchoring effect. With POM imaging, the droplets should be observed as the Maltese cross, though such a cross-like image is not straightforward for the distinct bipolar and radial structures because both molecular orientations cause similar images particularly when the two

point defects of the bipolar structures are aligned along the beam axis.[22,23,28] The self-organized droplets are almost perfectly spherical due to the interfacial tension, and different sizes of the droplets were obtained by vigorous shaking of their colloidal solution. Diameters of the droplets were determined directly from image processing of their POM snapshots, and they were within a few hundred of nanometers to a few micrometers.

3. RESULTS

Due to their high refractive index, the droplets are highly polarizable and easily trapped by the focused laser beam. In Figure 1, panels (a) and (b) show POM images for a ∼2.5 μm sized droplet upon irradiation by a linearly polarized beam with different power densities. We found that laser powers of few tens of MW/cm^2 are enough to trap the droplet stably in the focal spot, as reported by several groups in various contexts.[23,28,35,36] Under the trapping condition, the Maltese cross stays unchanged, indicating that the intrinsic configuration inside of the droplet apparently remains intact. When the laser power was increased to few hundreds of MW/cm^2, we observed that the POM images of the trapped droplet were time-dependent; the pattern of the Maltese cross disappeared, followed by the pattern of the rings, as shown in Figure 1b. Typically, a small ring near the center and one or two larger concentric rings showed up clearly on time scales of seconds to a few tens of seconds depending on the laser power. Such time evolution of POM images indicates unambiguously that reordering inside of the optically trapped droplet takes place under the high power of the laser beam. Upon the reordering, one notes that tiny fluctuations of the droplet diameter were observed. It is also important to stress that the transmittances

of ring patterns are highly decayed or diminished, suggesting a dramatic reduction in the droplet birefringence.

Figure 1c–e shows the POM images for a ~3.5 μm sized droplet optically trapped by a circularly polarized laser beam at different powers. Notably, at low laser powers, the optically trapped droplets are observed as a full-bright circular area in the POM images, as shown in Figure 1c. As the image is a 33 ms time-averaged picture, the full-bright circular area indicates the high-frequency rotating droplet, giving uniform aspect on the snapshot of the crossed-polarization light imaging. Associated with this consideration, the droplet rotates continuously without stopping within our observation window of 90 s. To demonstrate the rotation, we observed the orbit of a small droplet around the rotating droplet, as shown in Figure 1d. At high laser powers, the full-bright circular area was observed temporarily, indicating that the droplet rotates discontinuously. As shown in Figure 1e, when the full-bright circular area disappeared, darker ring patterns were observed similarly to those of a droplet trapped by the linearly polarized light. The reordering takes place in a few hundreds of milliseconds, and at the reordering state, the droplet is no longer rotated.

For both linearly and circularly polarized beams above the threshold, a higher laser power induces a faster reordering. When the laser beam was switched off, the ring patterns vanished immediately on the time scale of tens of milliseconds, irrespective of the laser trapping power, restoring the pattern related to the initial configuration inside of the droplet. Such an immediate restoration indicates that the recovery of the nematic configuration occurs without optical memory, hysteresis, or storage effects. In this context, we can consider that, when the optically controlled reorientation was removed, the anchoring effect at the droplet–liquid interface readily controlled the orientations of LC molecules on the surface and the internal ordering.

By varying the laser power to trap an individual LC droplet, we found that there is a clear threshold power, above which the optical trapping is followed by reordering throughout the inside of the droplet, as indicated by the formation of ring patterns with or without prior rotations. To evaluate the dependence of the threshold power on the droplet size and polarization state, we have performed and repeated the laser trapping experiments for different sizes of LC droplets by both linearly and circularly polarized beams. We found that the threshold is higher for a larger droplet. As far as reordering is considered, the threshold for a circularly polarized laser beam tends to be only slightly larger than that for a linearly polarized beam, as shown by the plot of the threshold as a function of $1/\Delta$ (where $\Delta = 2w_0/D$ is the ratio between the beam diameter ($2w_0$) and the droplet diameter (D) and w_0 is the beam waist at the focal plane) in Figure 2.

4. DISCUSSION

An interesting feature of the LC trapping experiment in this study is the optically induced reordering throughout the inside of the nematic LC droplet at high laser powers. To interpret this fact, we should consider OFT phenomena by the finite beam size of tightly focused light impinging on the LC thin films, in which the optical transition should occur when the free energy by the light field exceeds the Frank distortional energy. In the corresponding LC thin films, the transverse reorientation driven by optical nonlinearities has been analytically and accurately described.[19–21] In this case, the distribution of incident intensity of the beam $I(r)$ is considered. For an axial
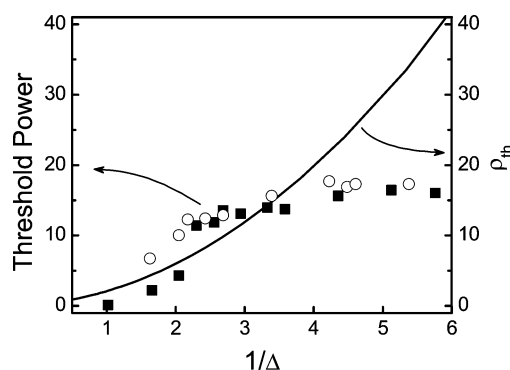

Figure 2. Plots of the experimentally observed threshold laser power density to induce the reordering in the optically trapped droplet (left y-axis; in $\times 10 + 200$ MW/cm^2) and the normalized intensity of the polarization-insensitive OFT threshold ρ_{th} (right y-axis; in MW/cm^2) as a function of $1/\Delta$. Data points denoted with filled rectangles and open circles are for linearly and circularly polarized beams, respectively.

symmetric Gaussian beam, the incident power and intensity of the beam are correlated by $P_0 = 2\pi \int_0^\infty I(r)\,dr = (\pi w_0^2/2)I_0$, where P_0 and I_0 is the incident power and intensity of the beam at the focal center, respectively. On the other hand, the intensity of the OFT threshold in the limit of the infinite plane wave approximation for a homeotropic alignment of LC thin films can be expressed as $I_\infty = \pi^2 c K n_e^2/d^2 n_o(n_e^2 - n_o^2)$,[37,38] where c denotes the speed of light, d is the thickness of the LC film, n_e and n_o are the extraordinary and ordinary refractive indices, and K is the average Frank elastic constant. The key feature of the OFT in the finite beam size approximation is that the threshold is determined by the ratio $\delta = 2w_0/d$ between the beam diameter and the cell thickness.[20,21] The normalized intensity of the OFT (defined as the ratio $\rho = I_0/I_\infty$) has been analytically and experimentally evaluated in terms of the beam diameter and the cell thickness,[19–21] and the normalized intensity of the OFT threshold ρ_{th} can be written as[21]

$$\rho_{th} = \left(1 + \frac{2^{3/2}}{\pi\delta}\right)^2 \tag{1}$$

By this quantitative point of view and by considering that the diameter of the droplet is approximately equal to the thickness of the LC thin film ($\Delta \approx \delta$), in Figure 2, we show the polarization-insensitive plot of ρ_{th} as a function of $1/\Delta$. As in this case w_0 is constant, the plot actually represents the dependence of the OFT threshold on the droplet size. The important finding is that the theoretical prediction is in agreement with the experimental observation, in which a larger OFT threshold power is required for a larger size of droplet, although the estimated intensity threshold values are lower than those observed in the experiments. For instance, a 2.5 μm droplet (which is considered as a 2.5 μm thin film with $K \cong 10$ pN) was estimated to have an intensity of the OFT threshold that is approximately 24 MW/cm^2, whereas the experimental value is ~360 MW/cm^2. Noting that the droplets are curved or bounded in the transverse plane, distinct to the corresponding planar thin films, it is qualitatively reasonable that the threshold intensity should be larger than the equivalent thin film accounting for finite beam size effects. The results also clearly indicate that the OFT film models have their limits when compared to a three-dimensional object such as the LC droplets.

4538

dx.doi.org/10.1021/jp308596h | *J. Phys. Chem. B* 2013, 117, 4536–4540

We recall that, as compared to the linearly polarized beam, the circularly polarized beam induces only a slightly higher or almost the same threshold for the same droplet size. This tends to prove that light polarization is not the reorientation nature because polarization dependence is basically expected in the OFT description. From the experimental data, thermal effects due to laser heating are likely involved in the laser-trapping-induced reconfiguration of the LC droplets. The decayed transmittance of the probe light also indicates a partial transition to an isotropic state due to strong thermal effects, convection, or deorientation. Further evaluations on those effects, particularly the thermal effect in the reordering, is desirable.

For the droplets with a diameter much larger than the beam diameter, the theoretical prediction shows a larger increase than that of the experimental observation. This fairly indicates that the anisotropic director may change drastically upon different sizes of droplets, resulting in such a deviation. The other possible reason is that the optical reorientation of the LCs is coupled with cooperative effects through dipolar interaction, which may reduce the threshold power as cooperative effects in the LC thin slab film result in a significant reduction of the critical electric field at which the OFT effect takes place.[39]

Upon reordering of the droplet, the configuration of LC molecules is still an open question. It is most probably an equilibrium reorientation of LC molecules throughout the inside of the droplet, although we consider that, as an anchoring surface, the molecular alignment at the interfacial layer should always remain intact. Though the surface anchoring can always control the molecular ordering as well as the coalescence and separation of the droplets,[40] such a boundary condition is involved in deformations represented by their Frank constants when dealing with the Fréederickscz transitions. We may note that because the birefringence and symmetry inside of the optically trapped droplet are modified by the reordering, the droplet center is spatially displaced with respect to the focal center, and it is rotated due to an unbalanced amount of angular momentum particularly when the beam was operated in the circular polarization. The tiny fluctuations of the droplet size upon the reordering can be a clear indication for the axial displacement under the linearly polarized beam, though one could also consider that it can be due to the geometrical modification of the trapped droplet. In comparison, such an axial displacement of an optically trapped smectic droplet occurs under the laser trapping condition.[28,36]

5. CONCLUSIONS

We have presented laser-trapping-induced reconfiguration of micrometer-sized bipolar nematic droplets of a liquid crystal dispersed in D_2O. The definite threshold laser power to induce such a reconfiguration depends on the droplet size and polarization state. The droplet size dependence can be explained by considering the nonlocal optical trapping-induced reorientations, the so-called optical Fréederickscz transitions, of the nematic LC droplet. With the finite size approximation, we show that the calculated threshold power as a function of droplet size is in qualitative agreement with the experimental data.

■ AUTHOR INFORMATION

Corresponding Author
*E-mail: usman@faculty.nctu.edu.tw (A.U.); masuhara@masuhara.jp (H.M.).

Notes
The authors declare no competing financial interest.

■ ACKNOWLEDGMENTS

■ REFERENCES

(1) Ashkin, A. *Phys. Rev. Lett.* **1970**, 24, 156−159.
(2) Ashkin, A. *Proc. Natl. Acad. Sci. U.S.A.* **1997**, 94, 4853−4860.
(3) Ashkin, A.; Dziedzic, J. M.; Bjorkholm, J. E.; Chu, S. *Opt. Lett.* **1986**, 11, 288−290.
(4) Sasaki, K.; Koshioka, M.; Misawa, H.; Kitamura, N.; Masuhara, H. *Jpn. J. Appl. Phys.* **1991**, 30, L907−L909.
(5) Urban, A. S.; Lutich, A. A.; Stefani, F. D.; Feldmann, J. *Nano Lett.* **2010**, 10, 4794−4798.
(6) Neuman, K. C.; Block, S. M. *Rev. Sci. Instrum.* **2004**, 75, 2787−2809.
(7) Bartlett, P.; Henderson, S. *J. Phys.: Condens. Matter* **2002**, 14, 7757−7768.
(8) Ito, S.; Tanaka, Y.; Yoshikawa, H.; Ishibashi, Y.; Miyasaka, H.; Masuhara, H. *J. Am. Chem. Soc.* **2011**, 113, 14472−14475.
(9) Sugiyama, T.; Adachi, T.; Masuhara, H. *Chem. Lett.* **2007**, 36, 1480−1481.
(10) Tsuboi, Y.; Shoji, T.; Kitamura, N. *J. Phys. Chem. C* **2010**, 114, 5589−5593.
(11) Masuhara, H.; Sugiyama, T.; Rungsimanon, T.; Yuyama, K.; Miura, A.; Tu, J.-R. *Pure Appl. Chem.* **2011**, 83, 869−883.
(12) Rungsimanon, T.; Yuyama, K.; Sugiyama, T.; Masuhara, H.; Tohnai, N.; Miyata, M. *J. Phys. Chem. Lett.* **2010**, 1, 599−603.
(13) Uwada, T.; Sugiyama, T.; Masuhara, H. *J. Photochem. Photobiol. A: Chemistry* **2011**, 221, 187−193.
(14) Sun, X.; Garetz, B. A.; Moreira, M. F.; Palffy-Muhoray, P. *Phys. Rev. E* **2009**, 79, 021701.
(15) Usman, A.; Uwada, T.; Masuhara, H. *J. Phys. Chem. C* **2011**, 115, 11906−11913.
(16) Erdmann, J. H.; Žumer, S.; Doane, J. W. *Phys. Rev. Lett.* **1990**, 64, 1907−1910.
(17) Doane, J. W.; Vaz, N. A.; Wu, B.-G.; Žumer, S. *Appl. Phys. Lett.* **1986**, 48, 269−271.
(18) Amundson, K. *Phys. Rev. E* **1996**, 53, 2412−2422.
(19) Khoo, I. C.; Liu, T. H.; Yan, P. Y. *J. Opt. Soc. Am. B* **1987**, 4, 115−120.
(20) Zolot́ko, A. S.; Kitieva, V. F.; Kuyumchyan, V. A.; Sobolev, N. N.; Sukhorukov, A. P. *JETP Lett.* **1982**, 36, 80−84.
(21) Brasselet, E.; Lherbier, A.; Dubé, L. J. *J. Opt. Soc. Am. B* **2006**, 23, 36−44.
(22) Juodkazis, S.; Shikata, M.; Takahashi, T.; Matsuo, S.; Misawa, H. *Appl. Phys. Lett.* **1999**, 74, 3627−3629.
(23) Juodkazis, S.; Matsuo, S.; Murazawa, N.; Hasegawa, I.; Misawa, H. *Appl. Phys. Lett.* **2003**, 82, 4657−4659.
(24) Wood, T. A.; Gleeson, H. F.; Dickinson, M. R.; Wright, A. J. *Appl. Phys. Lett.* **2004**, 84, 4292−4294.
(25) Gleeson, H. F.; Wood, T. A.; Dickinson, M. *Philos. Trans. R. Soc. London, Ser. A* **2006**, 364, 2789−2805.
(26) Yang, Y.; Brimicombe, P. D.; Roberts, N. W.; Dickinson, M. R.; Osipov, M.; Gleeson, H. F. *Opt. Express* **2008**, 16, 6877−6882.
(27) Brasselet, E.; Murazawa, N.; Juodkazis, S.; Misawa, H. *Phys. Rev. E* **2008**, 77, 041704.
(28) Brasselet, E.; Juodkazis, S. *J. Nonlinear Opt. Phys. Mater.* **2009**, 18, 167−194.
(29) Juodkazis, S.; Mukai, N.; Wakaki, R.; Yamaguchi, A.; Matsuo, S.; Misawa, H. *Nature* **2000**, 408, 178−181.

(30) Ito, S.; Sugiyama, T.; Toitani, N.; Katayama, G.; Miyasaka, H. *J. Phys. Chem. B* **2007**, *111*, 2365−2371.

(31) Durbin, S. D.; Arakelian, S. M.; Shen, Y. R. *Opt. Lett.* **1981**, *6*, 411−1414.

(32) Khoo, I. C.; Hou, J. Y.; Liu, T. H.; Yan, P. Y.; Michael, R. R.; Finn, G. M. *J. Opt. Soc. Am. B* **1987**, *4*, 886−891.

(33) de Gennes, P. G.; Prost, J. *The Physics of Liquid Crystals*, 2nd ed.; Clarendon Press: Oxford, U.K., 1993.

(34) Murazawa, N.; Juodkazis, S.; Misawa, H. *J. Phys. D* **2005**, *38*, 2923−2927.

(35) Murazawa, N.; Juodkazis, S.; Matsuo, S.; Misawa, H. *Small* **2005**, *1*, 656−661.

(36) Murazawa, N.; Juodkazis, S.; Misawa, H. *Eur. Phys. J. E* **2006**, *20*, 435−439.

(37) Palffy-Muhoray, P. In *Liquid Crystals: Applications and Uses*; Bahadur, B., Ed.; World Scientific: River Edge, NJ, 1990; Vol. *1*.

(38) Khoo, I. C.; Wu, S. T. *Optics and Nonlinear Optics of Liquid Crystals*; World Scientific: Singapore, 1993; Vol. *I*.

(39) Wang, X. Y.; Kyu, T.; Rudin, A. M.; Taylor, P. L. *Phys. Rev. E* **1998**, *58*, 5919−5922.

(40) Lavrentovich, O. D. *Liq. Cryst.* **1998**, *24*, 117−125.

4540

dx.doi.org/10.1021/jp308596h | *J. Phys. Chem. B* 2013, 117, 4536−4540